

# Characterization of Novel Diaryl Oxazole-Based Compounds as Potential Agents to Treat Pancreatic Cancer

Arthur Y. Shaw, Meredith C. Henderson, Gary Flynn, Betty Samulitis, Haiyong Han, Steve P. Stratton, H.-H. Sherry Chow, Laurence H. Hurley, and Robert T. Dorr

*The Arizona Cancer Center (M.C.H., B.S., S.P.S., H.-H.S.C., L.H.H., R.T.D.), the BIO5 Institute (G.F., L.H.H.), and the College of Pharmacy (A.Y.S., L.H.H.), University of Arizona, Tucson, Arizona; and the Translational Genomics Research Institute, Phoenix, Arizona (H.H.)*

Received May 19, 2009; accepted August 3, 2009

## ABSTRACT

A series of diaryl- and fluorenone-based analogs of the lead compound UA-62784 [4-(5-(4-methoxyphenyl)oxazol-2-yl)-9H-fluoren-9-one] was synthesized with the intention of improving upon the selective cytotoxicity of UA-62784 against human pancreatic cancer cell lines with a deletion of the tumor suppressor gene *deleted in pancreas cancer locus 4* (DPC-4, SMAD-4). Over 80 analogs were synthesized and tested for antitumor activity against pancreatic cancer (PC) cell lines (the PC series). Despite a structural relationship to UA-62784, which inhibits the mitotic kinesin centromere protein E (CENP-E), none of the analogs was selective for DPC-4-deleted pancreatic cancer cell lines. Furthermore, none of the analogs was a potent or selective inhibitor of four different mitotic kinesins (mitotic kinesin-5, CENP-E, mitotic kinesin-like protein-1, and mitotic centromere-associated kinesin). Therefore, other poten-

tial mechanisms of action were evaluated. A diaryl oxazole lead analog from this series, PC-046 [5-(4-methoxyphenyl)-2-(3-(3-methoxyphenyl)pyridin-4-yl) oxazole], was shown to potently inhibit several protein kinases that are overexpressed in human pancreatic cancers, including tyrosine receptor kinase B, interleukin-1 receptor-associated kinase-4, and proto-oncogene Pim-1. Cells exposed to PC-046 exhibit a cell cycle block in the S-phase followed by apoptotic death and necrosis. PC-046 effectively reduced MiaPaca-2 tumor growth in severe combined immunodeficiency mice by 80% compared with untreated controls. The plasma half-life was 7.5 h, and cytotoxic drug concentrations of  $>3 \mu\text{M}$  were achieved in vivo in mice. The diaryl oxazole series of compounds represent a new chemical class of anticancer agents that inhibit several types of cancer-relevant protein kinases.

Pancreatic cancer is the fourth leading cause of death from cancer in North America (Jemal et al., 2008). There are two agents approved in the United States for the treatment of metastatic pancreas cancer: 1) the cytidine analog gemcitabine and 2) the epidermal growth factor receptor inhibitor erlotinib (Tarceva) (Burris and Rocha-Lima, 2008). Neither drug alone or in combination is curative, and only incremental improvements in survival are produced by these agents

(Burris and Rocha-Lima, 2008). Whereas many other anticancer agents have been explored in the treatment of metastatic pancreatic cancer, none has yet proven to be effective. Thus, new agents with novel mechanisms of action are needed to treat metastatic pancreatic adenocarcinoma, which is the most commonly diagnosed stage of this disease.

The original intent of the chemistry campaign in this project was to develop analogs of a lead molecule UA-62784 that had showed modest selectivity for human pancreatic cancer cells with the *deleted in pancreas cancer locus 4* (DPC-4) gene deletion (Henderson et al., 2009). The DPC-4 deletion interrupts tumor suppression mediated by transforming growth factor- $\beta$  signaling (Jones et al., 2008), and more than half of pancreatic cancers have DPC-4 deletions (Jaffe et al., 2002; Miyaki and Kuroki, 2003). This is associated with decreased survival com-

This work was funded by the National Institutes of Health National Cancer Institute [Grant CA109552] (to D. D. Von Hoff of the Translational Genomics Research Institute, Phoenix, AZ).

A.Y.S. and M.C.H. contributed equally to this work.

Article, publication date, and citation information can be found at <http://jpet.aspetjournals.org>.  
doi:10.1124/jpet.109.156406.

**ABBREVIATIONS:** SAR, structure-activity relationship; DPC-4, deleted in pancreas cancer locus 4; PC, pancreatic cancer; SMAD-4, mothers against DPP homologs-4; Eg5, mitotic kinesin-5; CENP-E, centromere binding protein E; MKLP-1, mitotic kinesin-like protein-1; MCAK, mitotic centromere-associated kinesin; KIF3C, kinesin family member-3; TrkB, tyrosine receptor kinase B; IRAK-4, interleukin-1 receptor-associated kinase-4; PIM-1, proto-oncogene Pim-1; PDGFR, platelet-derived growth factor receptor; SCID, severe combined immunodeficiency; STR, short tandem repeat; PCR, polymerase chain reaction; DMSO, dimethyl sulfoxide; PI, propidium iodide; AUC, area under the curve; LC, liquid chromatography; MS, mass spectrometry; RED, rapid equilibrium dialysis; EDC, 1-ethyl-3-(3-dimethylaminopropyl)carbodiimide; DIEA, *N,N*-diisopropylethylamine; DCM, dichloromethane; DMF, *N,N*-dimethylformamide.

pared with those patients with wild-type *DPC-4* status (Tascilar et al., 2001). Because the lead molecule UA-62784 was shown to be an inhibitor of the mitotic kinesin, centromere-binding protein-E (CENP-E), a group of four mitotic kinesins, including CENP-E, were selected to evaluate newly synthesized analogs of UA-62784 for kinesin inhibitory activity. However, despite the structural relationship to the fluorenone-based UA-62784, none of the 80+ analogs synthesized showed selectivity for *DPC-4*-deleted human pancreatic cancer cells, sparking a search for other mechanisms of action. A result of this search showed that the most potent analog developed in this pancreatic cancer (PC) series, PC-046, was targeting a diverse group of protein kinases with relevance to cancer. In addition, PC-046 was active in SCID mice bearing human pancreas cancer, suggesting that the diaryl oxazole compounds in this series represent a new chemical class of anticancer agents, which have antitumor efficacy *in vivo*.

## Materials and Methods

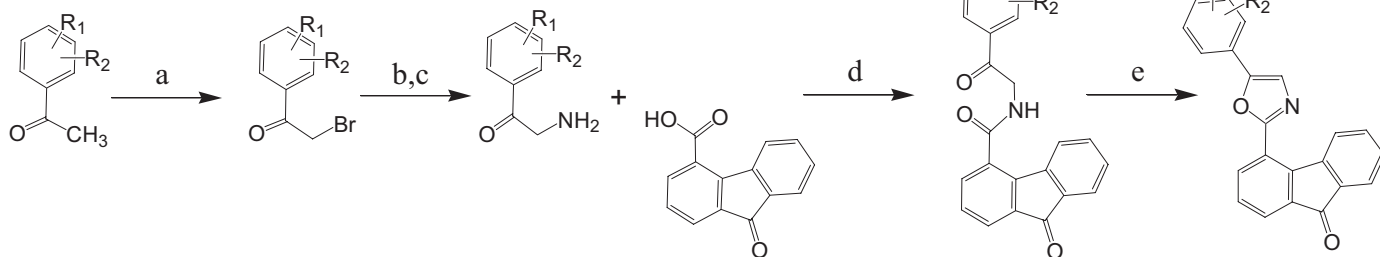
**Chemistry.**  $^1\text{H}$  and  $^{13}\text{C}$  NMR spectra were measured at 300 MHz on a Bruker 300-MHz NMR spectrometer. Chemical shifts were reported relative to internal  $\text{CDCl}_3$  ( $^1\text{H}$ , 7.26 ppm;  $^{13}\text{C}$ , 77.0 ppm) and  $\text{CD}_3\text{OD}$  ( $^1\text{H}$ , 3.30 ppm;  $^{13}\text{C}$ , 49.2 ppm). Flash-column chromatography was performed on Silica Gel 60 (35–75  $\mu\text{m}$ ), and thin-layer chromatography was performed on Silica Gel 60 F254 aluminum sheets. Melting points were determined on an electrothermal melting apparatus. High-resolution mass spectrometry spectra were recorded using electrospray ionization or matrix-assisted laser desorption ionization/time-of-flight techniques at the University of Arizona Mass Spectrometry Core Facility (Chemistry Department, Tucson, AZ).

**Chemicals.** The two synthetic approaches used to prepare 2,5-diaryl oxazole compounds are outlined in Fig. 1. The 2-bromoacetophenone and 2-aminoacetophenone intermediates were either available from commercial sources or prepared by bromination of commercial acetophenone precursors with *N*-bromosuccinimide (Guha et al., 2006) and, as required, subsequent displacement of the resulting 2-bromoacetophenone with sodium azide and phosphene reduction to provide the corresponding 2-aminoacetophenone tosylate salt (Holub et al., 2004). Direct coupling of the appropriate 2-aminoacetophenone salts to commercially available carboxylic acids followed by a Robinson-Gabriel cyclodehydration of the resulting ketoamide with phosphorous oxychloride (Nicolaou et al., 2004) was used to prepare many initial UA-62784 analogs (Fig. 1, Route 1). In a second more flexible approach (Route 2), palladium-catalyzed coupling of commercially available aryl boronic acids to a common 2-(2-bromoaryl) oxazole intermediate was used to efficiently prepare a large series of 2-biaryl-oxazole analogs (Meanwell et al., 1993). Preparation of PC-033, PC-032, and PC-046 as described below illustrates this general procedure (Fig. 2).

A mixture of 2-amino-4'-methoxyacetophenone hydrochloride (5.0 g, 22.32 mmol; Sigma-Aldrich, St. Louis, MO), 3-bromo-4-pyridinecarboxylic acid (4.96 g, 24.55 mmol; Matrix Scientific, Columbia, SC), EDC (5.12 g, 26.8 mmol), and DIEA (7.77 ml, 44.6 mmol) was dissolved in DCM (120 ml). The reaction mixture was stirred at 22°C for 18 h. The mixture was washed with 1 N NaOH, 0.2 N HCl, and brine. The organic layer was dried over  $\text{MgSO}_4$ , evaporated *in vacuo*, and then purified by column chromatography on silica gel (DCM/ethyl acetate = 3/1) to obtain PC-033 (3.25 g, 9.31 mmol, 41.7% yield).  $^1\text{H}$  NMR (300 MHz,  $\text{CDCl}_3$ ) 3.89 (s, 3 H), 7.06 (d,  $J$  = 9.0 Hz, 2 H), 7.58 (d,  $J$  = 4.8 Hz, 1 H), 8.05 (d,  $J$  = 9.0 Hz, 2 H), 8.62 (d,  $J$  = 4.8 Hz, 1 H), 8.79 (s, 1 H) ppm.

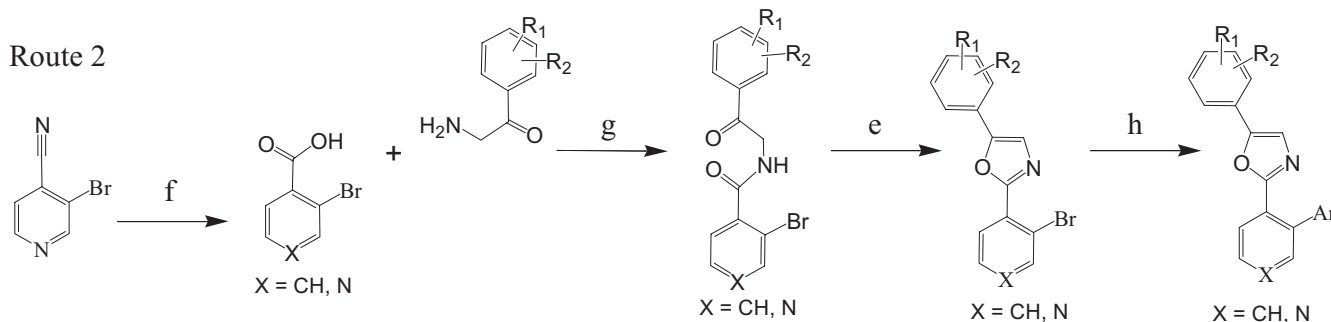
A mixture of PC-033 (3.25 g, 9.31 mmol) and phosphorus oxychloride (1.784 ml, 18.62 mmol) in DMF (10 ml) was stirred at 80°C for 2 h. The reaction solution was cooled to 22°C and diluted with ethyl

### Route 1



### Fluorenone Series

### Route 2



### Biaryl-Series

**Fig. 1.** Synthetic approaches to diaryl oxazoles. a, *N*-bromosuccinimide, trimethylsilyl trifluoromethanesulfonate. b,  $\text{NaN}_3$ , DMSO, 30 min rt. c,  $\text{PPh}_3$ , TsOH, tetrahydrofuran, 24 h. d, EDC, DIEA, DCM. e,  $\text{POCl}_3/\text{DMF}$  (1:5), 80°C, 2 h. f,  $\text{Ar-B(OH)}_2$ ,  $\text{Pd(PPh}_3)_4$ ,  $\text{Na}_2\text{CO}_3$ ,  $\text{DME}/\text{H}_2\text{O}$  (3:1), reflux, 2 h.

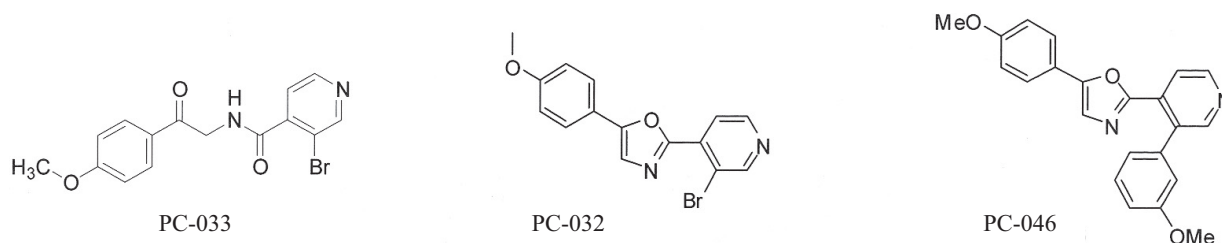


Fig. 2. Structures of PC-032, PC-033, PC-046.

acetate (10 ml) and washed with water twice at 10 ml. The organic layer was dried over  $\text{MgSO}_4$ , evaporated in vacuo, and purified by column chromatography on silica gel (DCM/ethyl acetate = 3/1) to obtain PC-032 (2.7g, 8.15 mmol, 88% yield).  $^1\text{H}$  NMR (300 MHz,  $\text{CDCl}_3$ ), 3.71 (s, 3 H), 6.86 (d,  $J = 9.0$  Hz, 2 H), 7.46 (s, 1 H), 7.58 (d,  $J = 9.0$  Hz, 2 H), 8.22 (d,  $J = 6.0$  Hz, 1 H), 8.55 (d,  $J = 6.0$  Hz, 1 H), 8.87 (s, 1 H) ppm.  $^{13}\text{C}$  NMR (75 MHz,  $\text{CDCl}_3$ ) 55.38, 114.81, 116.84, 118.53, 124.07, 125.11, 126.84, 140.03, 141.09, 148.03, 154.39, 155.76, 161.32 ppm. High-resolution mass spectrometry ( $\text{M} + \text{H}^+$ ) calculated for  $\text{C}_{15}\text{H}_{12}\text{BrN}_2\text{O}_2$  331.0082; found 331.0070.

PC-032 (0.15 g, 0.453 mmol), 3-methoxyphenylboronic acid (0.138 g, 0.906 mmol), tetrakis(triphenylphosphine) palladium (0.026 g, 0.023 mmol), and sodium carbonate (0.144 g, 1.359 mmol) were stirred in DME/ $\text{H}_2\text{O}$  (9 ml/3 ml) under argon atmosphere at reflux for 2 h. The reaction mixture was diluted with ethyl acetate (10 ml) and washed with water and brine. The organic layer was dried over  $\text{MgSO}_4$  and evaporated in vacuo to obtain the crude product. Further purification by gradient silica gel chromatography (hexane/ethyl acetate = 3/1 to 1/2) afforded PC-046 (0.143g, 0.399 mmol, 88% yield).  $^1\text{H}$  NMR (300 MHz,  $\text{CDCl}_3$ ) 3.81 (s, 3 H), 3.84 (s, 3 H), 6.83 (d,  $J = 2.1$  Hz, 1 H), 6.87 (d,  $J = 2.7$  Hz, 1 H), 6.95–6.97 (m, 2 H), 7.03 (dd,  $J = 2.7, 1.5$  Hz, 1 H), 7.15 (dd,  $J = 6.9, 2.1$  Hz, 2 H), 7.29 (d,  $J = 6.9$  Hz, 1 H), 7.39 (t,  $J = 7.8$  Hz, 1 H), 8.04 (d,  $J = 5.1$  Hz, 1 H), 8.69 (s, 1 H), 8.73 (d,  $J = 5.1$  Hz, 1 H) ppm.  $^{13}\text{C}$  NMR (75 MHz,  $\text{CDCl}_3$ ) 55.75, 55.78, 113.98, 114.67, 115.14, 120.48, 122.11, 122.26, 126.18, 129.77, 133.07, 135.23, 139.97, 149.32, 152.21, 152.88, 158.61, 159.94, 160.49 ppm. HRMS ( $\text{M} + \text{H}^+$ ) calculated for  $\text{C}_{22}\text{H}_{18}\text{N}_2\text{O}_3$  359.1396; found 359.1392.

**Cell lines and Culture Conditions.** Human pancreatic cancer cell lines MiaPaCa-2 (Yunis et al., 1977), Panc-1 (Lieber et al., 1975), and BxPC3 (Tan et al., 1986) were purchased from the American Type Culture Collection (Manassas, VA) and cultured in a humidified incubator at 37°C, 5%  $\text{CO}_2$ , in RPMI 1640 medium (CellGro, Manassas, VA) supplemented with 10% heat-inactivated bovine calf serum, 2 mM L-glutamine, 100 U/ml penicillin, and 100  $\mu\text{g}/\text{ml}$  streptomycin (Invitrogen, Carlsbad, CA). MiaPaCa-2 (CRL-1420) is an adherent epithelial human pancreatic cancer cell line with a doubling time of approximately 40 h (Yunis et al., 1977). Panc-1 (CRL-1469) is an undifferentiated human pancreatic epithelial cell line with a doubling time of approximately 52 h (Lieber et al., 1975). The BxPC3 cell line *DPC-4*( $-/-$ ) and its isogenic restored wild-type *DPC-4*( $+/+$ ) cell line were developed and cultured as described previously (Wang et al., 2006). In brief, a *DPC-4*-expressing construct (pMSCVneo*DPC-4*) was created by amplifying full-length cDNA of *DPC-4* using reverse transcriptase-PCR and subcloning into the multiple cloning site of a retroviral vector (pMSCVneo). The *DPC-4*-expressing construct was cotransfected into the BxPC3 *DPC-4*( $-/-$ ) cells using a packaging cell line, resulting in a cell line that constitutively expresses *DPC-4*. The expression of *DPC-4* was confirmed by Western blotting (Wang et al., 2006).

**Verification of Cell Line Identities.** Cell line identities were verified by STR profiling (Collins et al., 2004) by the Human Origins Genotyping Laboratory at the University of Arizona, using the AmpFISTR Identifier PCR amplification kit (Applied Biosystems, Foster City, CA). This method simultaneously amplifies 15 STR loci and amelogenin in a single tube, using five dyes, 6-carboxyfluorescein,

2',7'-dimethyl-oxy 4'5'-dichloro 6-carboxyfluorescein, NED, PET, and LIZ, which are then separated on a 3730 Genetic Analyzer (Applied Biosystems). GeneMarker, version 1.7, software was used for analysis (Soft Genetics, State College, PA). AmpFISTR control DNA and the AmpFISTR allelic ladder were run concurrently. Results were compared to published STR sequences from the American Type Culture Collection.

**Cytotoxicity Assays.** Cytotoxicity assays in the mechanism of action studies were performed according to Mosmann (1983), wherein the activity of mitochondrial reductases were measured using 3-(4,5-dimethylthiazol-3-yl)-2,5-diphenyltetrazolium bromide dye. In brief, cells were seeded in 96-well plates and incubated for various times at 37°C. Inhibition of cell growth was measured by adding 3-(4,5-dimethylthiazol-3-yl)-2,5-diphenyltetrazolium bromide dye, and after an additional 4 h of incubation at 37°C, the 96-well plates were centrifuged, and the culture supernatant was removed. DMSO was added to each well to solubilize the formazan crystals, and the optical density was read at 540 nm on a  $\mu\text{Quant}$  Spectrophotometer (BioTek Instruments, Winooski, VT). Cell growth inhibition data are expressed as percentage of survival compared with untreated cells. The  $\text{IC}_{50}$  is defined as the drug concentration required to produce 50% growth inhibition. Results are mean  $\pm$  S.E.M. ( $n = 3$ ).

**Preparation of PC-046.** For in vitro studies, a 50 mM stock solution of PC-046 was prepared in DMSO and subsequently diluted into cell culture medium at working concentrations, ensuring that the final DMSO concentration used in cell culture is less than 0.1%, which we have previously determined to have no cytotoxic effect on our cell lines. For in vivo studies, PC-046 was prepared in 88% DMSO, 10% Tween 80, and 2% benzyl alcohol.

**Kinesin ATPase Assay.** The colorimetric kinesin ATPase assay was purchased from Cytoskeleton, Inc. (Denver, CO) and performed as indicated by the manufacturer (Funk et al., 2004). In short, 0.2 to 1.0  $\mu\text{g}$  of purified recombinant CENP-E (Yen et al., 1991; Lombillo et al., 1995), Eg5/kinesin spindle protein (Sawin et al., 1992), MCAK (Hunter et al., 2003), and MLKP-1 (Nislow et al., 1992) mitotic kinesin motor proteins and the nonmitotic KIF3C kinesin (Yang and Goldstein, 1998) were added to paclitaxel-stabilized microtubules in a 96-well plate. Increasing amounts of UA-62784 or PC analogs were added to the wells before the addition of ATP (Sigma-Aldrich), and the reaction was incubated at 22°C for 5 min. The CytoPhos reagent (Cytoskeleton Inc.) was added to halt the reaction, and color was allowed to develop for 10 min. Absorbance at 650 nm was measured in a  $\mu\text{Quant}$  Spectrophotometer (BioTek Instruments).

**Measurement of Cell Cycle.** The percentage of cells in different cell cycle phases of division was measured by flow cytometry (Darynski et al., 1996) using propidium iodide (PI) (Sigma-Aldrich). In brief, cells were treated with PC-046 for 24 to 72 h, fixed with 70% ethanol overnight, and then stained with 40  $\mu\text{g}/\text{ml}$  PI and 0.5 mg/ml RNase A for 30 min at 37°C. PI fluorescence was measured on a FACScan (BD Biosciences, San Jose, CA) and analyzed using Mod-Fit (Verify Software, Topsham, ME). Data are mean  $\pm$  S.E.M. ( $n = 3$ ).

**Measurement of Apoptosis and Necrosis.** Apoptosis and necrosis after PC-046 treatment was measured at 24 to 72 h by flow cytometry (Vermees et al., 1995) using Annexin V-Alexa Fluor 488 (Invitrogen) and propidium iodide (BioVision, Mountain View, CA).

Because of the greater photostability of Alexa Fluor 488 over fluorescein isothiocyanate, we substituted Alexa Fluor 488-labeled Annexin V for fluorescein isothiocyanate-labeled Annexin V. Apoptosis was measured by positive Annexin V staining, indicating the translocation of phosphatidylserine on the cell membrane of apoptotic cells, whereas necrosis was measured by dual labeling of Annexin V and propidium iodide of necrotic cells. Unstained cells were deemed alive. Fluorescence of Annexin V-Alexa Fluor 488 and PI was measured on FL1 and FL2, respectively, on a BD Biosciences FACScan using CellQuest Pro software (BD Biosciences). Data are mean  $\pm$  S.E.M. ( $n = 3$ ).

**Measurement of Macromolecular Synthesis.** Radiolabeled precursors of DNA ( $[^3\text{H}]$ thymidine) and protein ( $[^{14}\text{C}]$ valine) were obtained from GE Healthcare (Piscataway, NJ). The RNA precursor  $[^3\text{H}]$ uridine was obtained from MP Biomedical (Irvine, CA). In brief, cells were plated in 96-well plates and allowed to adhere before adding PC-046 for 24 to 72 h. Radiolabeled precursors ( $1 \mu\text{Ci}/\text{well}$  for thymidine and uridine, and  $0.05 \mu\text{Ci}/\text{well}$  for valine) were added and allowed to incorporate for 6 h at  $37^\circ\text{C}$ . Cells were harvested onto Unifilter-96 GF/B filterplates using a Packard Filtermate 96-well harvester and counted using a Packard Top Count NXT 96-well scintillation counter (PerkinElmer Life and Analytical Sciences, Boston, MA).

**In Vivo Studies.** Six- to 7-week-old male SCID mice were implanted with  $10 \times 10^6$  MiaPaCa-2 cells in MatriGel (BD Biosciences) subcutaneously in the flank to establish tumors. Once the tumors reached approximately  $100 \text{ mm}^3$  and were palpable (approximately 3 weeks later), PC-046 treatment was initiated. PC-046 was prepared in 88% DMSO, 10% Tween 80, and 2% benzyl alcohol. Mice were administered vehicle alone or 44, 55, or 66 mg/kg/day PC-046 intraperitoneally for 5 consecutive days. Tumor size, body weight, and general health of each mouse were recorded every 3rd day for the duration of the study.

**Kinase Screening.** Initial kinase screening was performed by Amphora Discovery Corporation (Durham, NC). Forty-eight protein kinases were screened using a  $10 \mu\text{M}$  concentration of 12 PC compounds or UA-62784 by measuring  $[^{33}\text{P}]$ ATP incorporation into a specific kinase substrate. Subsequent kinase screening and  $\text{IC}_{50}$  determination were performed by SignalChem Pharmaceuticals, Inc. (Richmond, BC, Canada) using a  $25 \mu\text{M}$  concentration of PC-046 (for the screening) and eight concentrations of PC-046 from 10 nM to  $50 \mu\text{M}$  for the dose-response curve.

**Pharmacokinetic Studies.** The pharmacokinetics of PC-046 in nontumor bearing SCID mice was determined after intravenous administration of a single dose of 88 mg/kg. Plasma samples were

collected at 0, 1, 5, 15, 30, 60, 90, 120, 240, 480, 960, and 1440 min after dosing. Plasma PC-046 concentrations were analyzed by reversed-phase chromatography and tandem mass spectrometry. In brief, mouse plasma was mixed with 99 volumes of acetonitrile, and an aliquot of the supernatant was injected onto the LC-MS. The LC-MS analysis was performed on a ThermoFinnigan Quantum Ultra triple quadrupole mass spectrometer (Thermo Fisher Scientific, Waltham, MA) in tandem with a Surveyor LC system. Chromatographic separation was achieved with a Luna  $\text{C}_{18}$  column ( $2 \times 50 \text{ mm}$ ,  $5 \mu$ ) (Phenomenex, Torrance, CA) and a mobile phase of 47.5% acetonitrile with 5 mM ammonium formate and 0.05% trifluoroacetic acid at a flow rate of 0.3 ml/min. Analytes were ionized by positive electrospray ionization and detected using selective reaction monitoring for transitions of 395/182 at a collision energy of 52 eV and 395/197 at a collision energy of 39 eV. The assay is linear over the range of 0.05 to  $5 \mu\text{g}/\text{ml}$  from  $10 \mu\text{l}$  of mouse plasma. The PC-046 concentration-time data [half-life, area under curve (AUC) of the plasma concentration-time profile, systemic clearance, and volume of distribution] were analyzed by the noncompartmental approach using WinNonlin, version 5.2 (Pharsight, Mountain View, CA). Data are mean  $\pm$  S.E.M. ( $n = 3$ ).

**Plasma Protein Binding.** Plasma protein binding of PC-046 was determined in human and mouse plasma using rapid equilibrium dialysis (RED) devices manufactured by Thermo Fisher Scientific. Plasma pH was adjusted to 7.4 and spiked with PC-046 to a final plasma concentration of  $1 \mu\text{g}/\text{ml}$ . Aliquots ( $500 \mu\text{l}$ ) of the spiked plasma were placed into the sample chamber, and  $750 \mu\text{l}$  of phosphate-buffered saline were placed into the adjacent chamber. Triplicate samples were loaded into the RED devices. The RED devices were incubated at  $37^\circ\text{C}$  on an orbital shaker operating at 100 rpm for 24 h. Preliminary studies were conducted to show that equilibrium is reached at 24 h and to confirm drug stability at  $37^\circ\text{C}$  for 24 h. After the incubation, aliquots of plasma and buffer were removed for the analysis of PC-046 concentration by LC-MS-MS as described above.

## Results

**Development of SAR for UA-62784 and Biaryl Analogs.** Because of its high potency against isogenic BxPC3 cell lines, UA-62784 was used as the starting point for the chemical synthesis campaign. The limitations of UA-62784 include a lack of solubility that relates to its high calculated partition coefficient ( $\text{Clog } P = 5.44$ ) and a relatively low (2-fold) selectivity index for BxPC3 DPC-4(-/-) cells. In addition

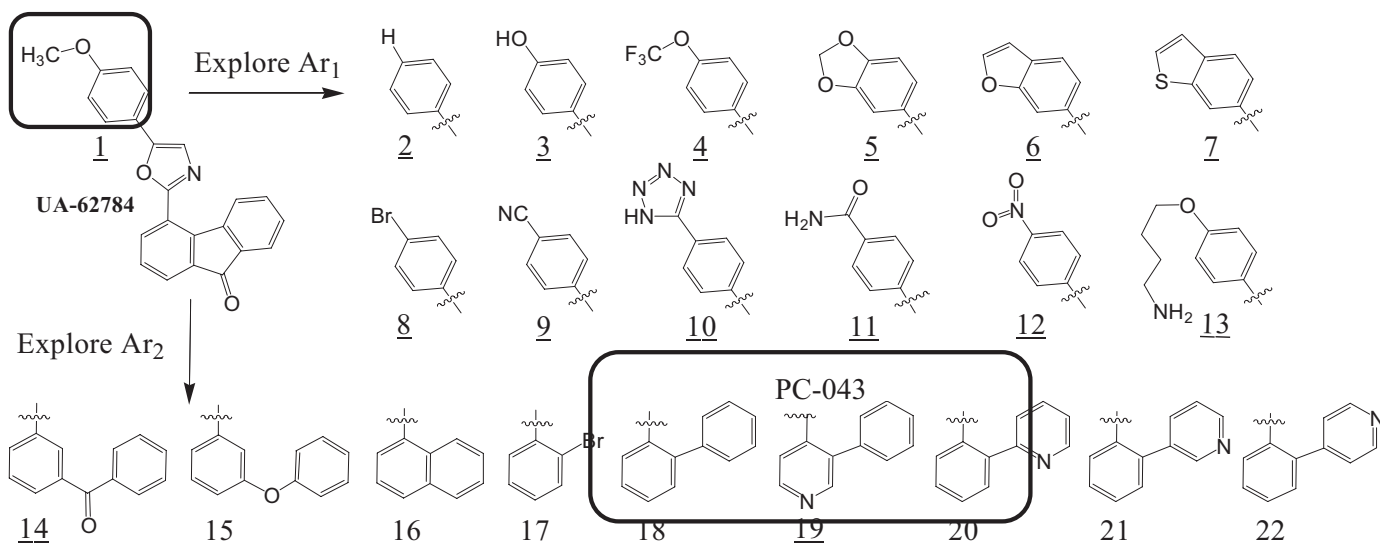
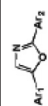
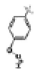

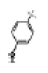


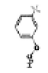

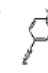



Fig. 3. SAR exploration of UA-62784 (PC-001) fluorenone series.



TABLE 1  
Summary of PC analogs with selected Ar1 modifications

Cmpd Code		Mol. Wt.	Clog P	$\mu\text{M}$			Eg5 IC <sub>50</sub> <sup>c</sup>	CENP-E IC <sub>50</sub> <sup>c</sup>	MKLP-1 IC <sub>50</sub> <sup>c</sup>	KIF3C IC <sub>50</sub> <sup>c</sup>	MCAK IC <sub>50</sub> <sup>c</sup>
				BxPC3 DPC-4(+/+) IC <sub>50</sub> <sup>a</sup>	BxPC3 DPC-4(-/-) IC <sub>50</sub> <sup>a</sup>	DPC-4 ± Selectivity Index <sup>b</sup>					
UA-62784 (PC-001)		353.37	5.44	0.023	0.012	>100	7.3	>100	>100	>100	
NS-44636 (PC-002)		323.34	5.43	5.3	2.8	>100	>100	>100	>100	>100	
PC-004		539.34	4.95	2.4	1.3	>100	>100	11.1	>100	>100	
PC-046		358.13	3.28	0.013	0.0075	>100	>100	>100	>100	>100	
PC-049		328.12	3.4	20	18	>100	>100	>100	>100	>100	
PC-053		358.13	3.28	3.5	3.5	>100	11	14	>100	>100	
PC-051		412.36	4.93	15	12	>100	>100	>100	>100	>100	
PC-050		353.37	3.44	>20	>20	>100	>100	>100	>100	>100	
PC-052		346.35	3.56	>20	>20	>100	>100	>100	>100	>100	


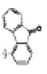
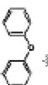


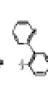
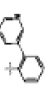

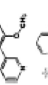
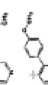

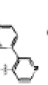
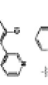

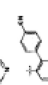
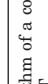


Cmpd Code, compound code; Clog P, logarithm of a compound's partition coefficient between *n*-octanol and water  $\log(c_{\text{octanol}}/c_{\text{water}})$  (i.e., a measurement of a compound's hydrophobicity).

<sup>a</sup> IC<sub>50</sub> values were determined by 96-h MTT.

<sup>b</sup> Ratio of IC<sub>50</sub>s of BxPC3 DPC-4(+/+):BxPC3 DPC-4(-/-).

<sup>c</sup> IC<sub>50</sub>s of selected compounds against various kinesin targets.

TABLE 2  
Summary of PC analogs with selected Ar2 modifications

Cmpd Code		Mol. Wt.	Clog P	BxPC3 $DPC-4(+/+)$ $IC_{50}^a$	BxPC3 $DPC-4(-/-)$ $IC_{50}^a$	$DPC-4$ $\pm$ Selectivity Index <sup>b</sup>	Eg5 $IC_{50}^c$	CENP-E $IC_{50}^c$	MKLP-1 $IC_{50}^c$	KIF3C $IC_{50}^c$	MCAK $IC_{50}^c$
$\mu M$											
UA-62784 (PC-001)		353.37	5.44	0.023	0.012	1.9	>100	7.3	>100	>100	>100
PC-024		343.38	6.13	53	43	1.23	>100	>100	>100	>100	39
PC-027		301.34	5.21	3.8	2.5	1.52	>100	>100	>100	>100	>100
PC-026		327.28	5.32	0.016	0.014	1.14	>100	>100	>100	>100	>100
PC-043		328.36	3.93	0.0068	0.0075	0.91	100	>100	>100	>100	>100
PC-045		328.36	3.83	0.023	0.023	1	>100	>100	>100	>100	>100
PC-039		328.36	3.83	0.03	0.03	1	>100	>100	>100	>100	100
PC-038		328.36	3.83	2.5	2.6	0.96	>100	>100	>100	>100	>100
PC-044		358.13	3.28	0.06	0.12	1.33	>100	>100	100	>100	100
PC-046		358.13	3.28	0.013	0.0075	1.73	>100	>100	>100	>100	>100
PC-047		358.13	3.28	0.2	0.2	1	>100	>100	>100	>100	>100
PC-042		329.35	2.49	0.38	0.38	1	>100	55	52	>100	>100
PC-055		346.35	3.56	0.11	0.093	0.12	>100	100	100	>100	>100
PC-056		362.81	3.96	0.36	0.31	1.16	>100	>100	>100	>100	>100
PC-057		362.81	3.96	0.086	0.08	1.08	>100	>100	71	>100	>100
PC-058		362.81	3.96	0.2	0.19	1.05	>100	>100	53	>100	>100
PC-054		353.37	3.44	>20	>20	1	>100	>100	>100	>100	>100

Cmpd Code, compound code; Clog P, logarithm of a compound's partition coefficient between *n*-octanol and water  $\log(c_{octanol}/c_{water})$  (i.e., a measurement of a compound's hydrophobicity).

<sup>a</sup>  $IC_{50}$  values were determined by 96-h MTT.

<sup>b</sup> Ratio of  $IC_{50}$ s of BxPC3  $DPC-4(+/+)$ :BxPC3  $DPC-4(-/-)$ .

<sup>c</sup>  $IC_{50}$ s of selected compounds against various kinesin targets.

to addressing these limitations, the analog studies were directed toward understanding the essential pharmacophore elements and the biological targets responsible for the growth-inhibitory effects. Keeping the oxazole core of UA-62784 constant, the two aryl substituents (Ar1 and Ar2) were systematically optimized for the fluorenone series (Fig. 3). Summary data for Ar1 SAR are listed in Table 1, and SAR data for Ar2 are listed in Table 2. It is a striking revelation that high potency against BxPC3 cell lines is only seen where Ar1 is 4-methoxy-phenyl (compounds PC-001 and PC-046). Even minor modifications, such as replacement of the 4-methoxy group with 4-hydroxy or 4-trifluoromethoxy at Ar1, are not well tolerated. These tight SAR observations suggest a specific target or a closely related class of targets as responsible for the observed cytotoxic activity. Therefore, Ar1 was held as 4-methoxy-phenyl, and the influence of the fluorenone Ar2 system was systematically explored (Table 2). The key pharmacophore elements for Ar2 were also quite specific with the 2-biaryl analog PC-026 (Table 2), the first variant that retained high potency. Subsequent biaryl analogs (PC-038, PC-039, PC-043, and PC-045) incorporated a pyridine ring in hopes of improving solubility (Table 2). Of these compounds, PC-043 and PC-045 retained potency. For ease of synthesis reasons, PC-043 was selected for further modification (Fig. 4). Three pyridylphenyl analogs were found to be potent in the low nanomolar range, with PC-046 being the most potent (Table 2). The selectivity index for different analogs was based on the ratio of the  $IC_{50}$  in BxPC3 *DPC-4*(+/+) to BxPC3 *DPC-4*(-/-) cells and ranged from 0.12 to 1.9 in this analog series. Indeed, all but one of the selectivity scores in this series are lower than the 1.9 for parent compound UA-62784 (Table 1, compound PC-001).

**Kinesin ATPase Inhibition.** Five different purified recombinant kinesin motor proteins were evaluated for inhibition by selected PC analogs. This included four mitotic kinesins, Eg5, CENP-E, MKLP-1, and MCAK, and the nonmitotic (neuronal) kinesin KIF3C (Hirokawa and Noda, 2008). These were characterized for ATPase inhibitory activity with the PC series. None of the 23 analogs selected for kinesin testing was inhibitory for the mitotic kinesin Eg5 or the neuronal kinesin KIF3C at concentrations up to 100  $\mu$ M (Tables 1 and 2). This upper concentration limit was always far greater than the cytotoxic  $IC_{50}$ s for each analog. It is interesting that only two analogs inhibited CENP-E; the  $IC_{50}$  for PC-042 (Table 2) was 55  $\mu$ M, and the  $IC_{50}$  for PC-053 (Table 1) was 11  $\mu$ M. Although the position of the methoxy substituent at Ar1 is different in both analogs, a 2-aryl-4-pyridryl moiety at Ar2 is a common feature. Likewise, only one analog, PC-024, inhibited MCAK, with an  $IC_{50}$  of 39  $\mu$ M (Table 2). The structure of PC-024 differs from the others by substitution of the 2-aryl-4-pyridryl moiety at Ar2, with a simple 4-phenoxyphenyl group. Analog PC-024 had the lowest overall cytotoxic potency for the 25 compounds tested for kinesin inhibition of the 23 analogs tested, with an  $IC_{50}$  = 43  $\mu$ M. In contrast, growth inhibitory potency in the BxPC3 cell line showed significant correlations with CENP-E and MKLP-1, albeit with low  $r^2$  values. For CENP-E, the  $r^2$  was 0.27 ( $p$  = 0.049) and, for MKLP-1, the  $r^2$  value was 0.23 ( $p$  = 0.038). Overall, there were little data to suggest that mitotic kinesins comprise the molecular targets of this group of compounds.

**Protein Kinase Inhibition.** Protein kinases play critical roles in all aspects of cellular metabolism: survival, proliferation, signaling, division, repair, and metastasis; so, it is no wonder that they are frequently activated in cancer. Thus, a compound that targets kinases can be a valuable tool in the

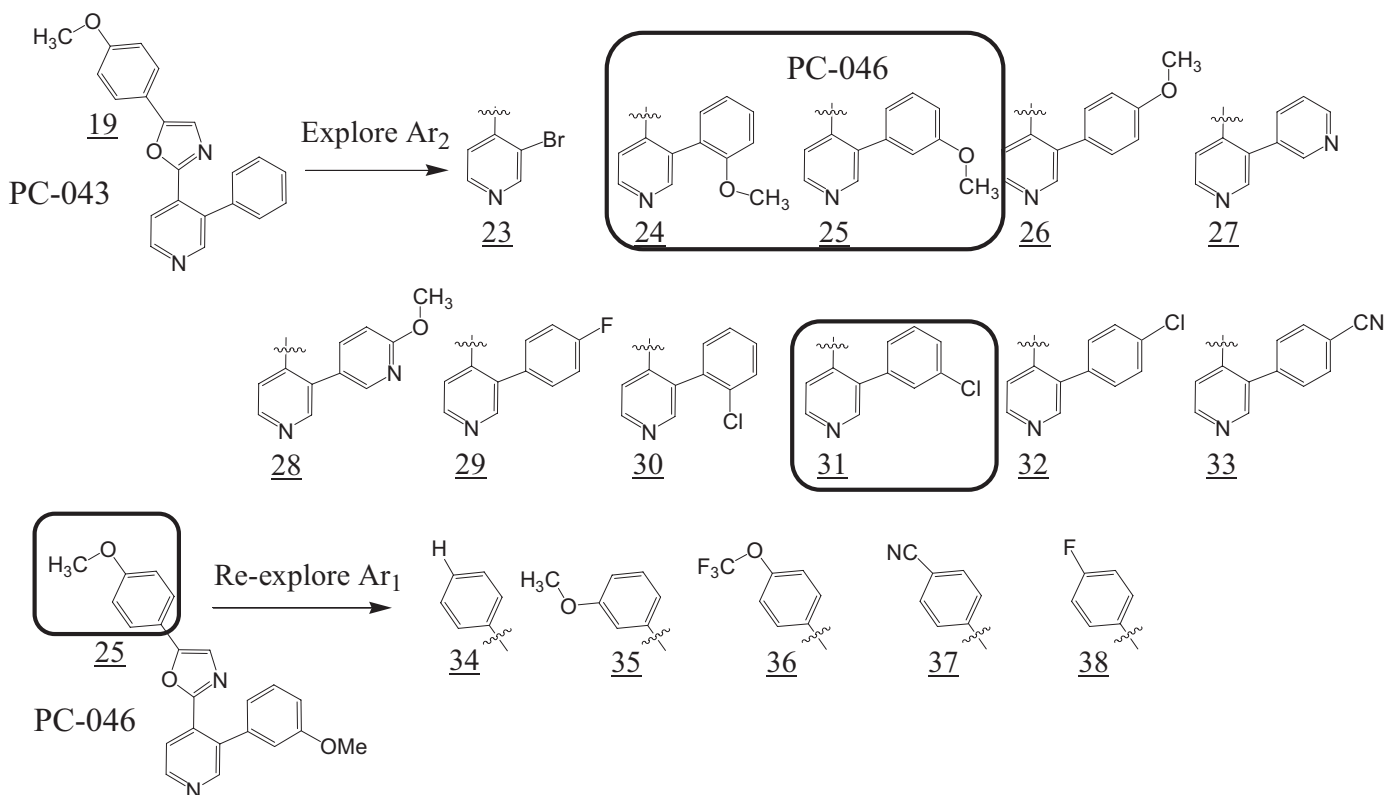
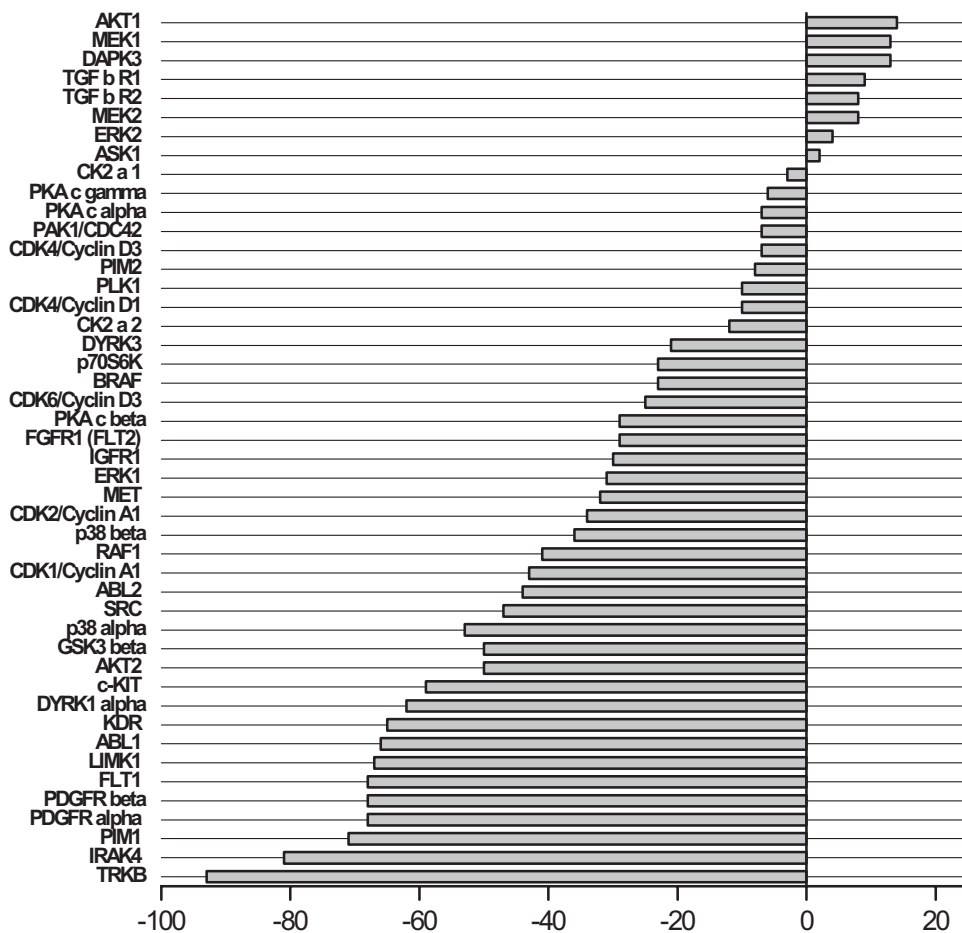


Fig. 4. SAR exploration of PC-043 diaryl oxazole series.

## Percent Activity Change with PC-046



**Fig. 5.** Kinase profiling summary. Kinase screening was performed using 25  $\mu$ M PC-046 in a cell-free in vitro kinase activity assay by measuring [ $^{33}$ P]ATP incorporation into a specific kinase substrate. The x-axis shows the percentage of change in activity against a specific kinase (y-axis).

oncologist's arsenal of treatment options. Because PC-046 demonstrated the greatest cytotoxicity against both *DPC-4*(+/+) and *DPC-4*(-/-) BxPC3 cells, this compound was further characterized for its kinase inhibitory activity. This analog retains the 4-methoxyphenyl side group at Ar1 and the oxazole core of UA-62784 but substitutes a 2-(*m*-methoxyphenyl)-4-pyridyl moiety for the fluorenone functionality at Ar2.

The initial screen of 48 protein kinases incubated with 12 compounds (10  $\mu$ M each) and UA-62784 showed >50% inhibition of CDK2/cyclin A for compounds PC-001 (57% inhibition), PC-002 (57% inhibition), and PC-004 (57% inhibition). There was no significant (>50%) inhibition of any protein kinases by compounds PC-024, PC-027, PC-102, PC-103, and UA-62784. Analog PC-026 inhibited PDGFR $\alpha$  (59% inhibition) and PDGFR $\beta$  (43% inhibition). The only compounds showing substantial multikinase inhibition were PC-043 and PC-046. Analog PC-043 produced nearly 50% inhibition of PIM-1 kinase and TrkB kinase, whereas PC-046 inhibited PIM-1 (50%), PDGFR $\alpha$  (46%), and TrkB (55%).

Based on these initial results, a follow-up screen was performed using 25  $\mu$ M PC-046, the standard drug concentration used by SignalChem Pharmaceuticals, Inc., for kinase inhibition assays. PC-046 inhibited three kinases by more than 70%: IRAK-4, PIM-1, and TrkB (Fig. 5). The IC<sub>50</sub> of these three kinases were measured using an eight-point concentration range from 10 nM to 50  $\mu$ M. The IC<sub>50</sub> values for

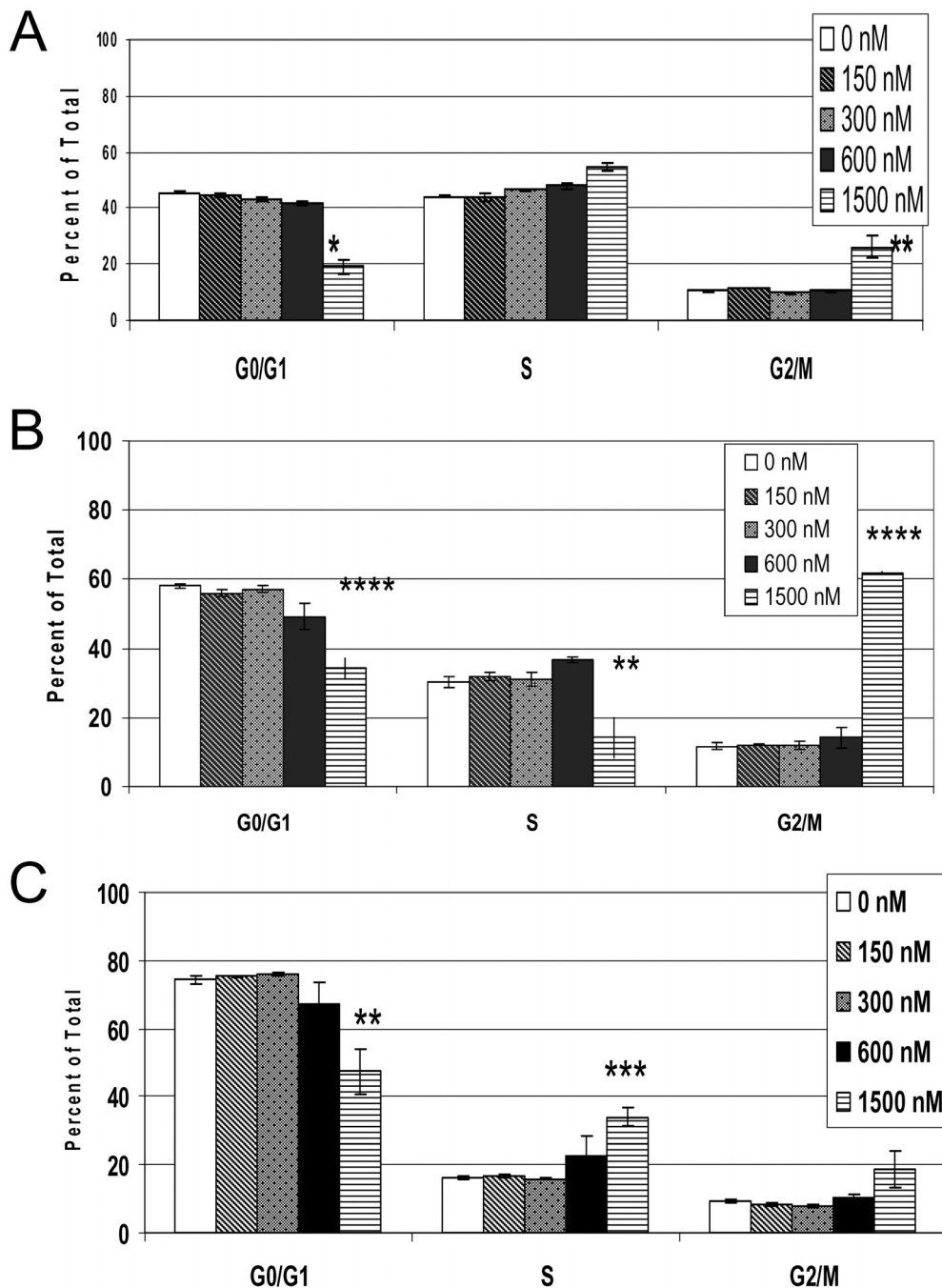
PC-046 generated from best-fit line graphs (all  $r^2 = 0.99$ ) were 13.4  $\mu$ M for TrkB, 15.4  $\mu$ M for IRAK-4, and 19.1  $\mu$ M for PIM-1. At the highest PC-046 concentration tested (50  $\mu$ M), inhibition of the respective kinases was TrkB (98%), IRAK-4 (92%), and PIM-1 (84%) (data not shown).

**Cell Cycle Arrest and Induction of Cell Death.** Cell cycle analyses showed a reduction in the percentage of G<sub>0</sub>/G<sub>1</sub>-phase cells and a commensurate increase in G<sub>2</sub>/M-phase cells (Fig. 6). We used Annexin V/PI staining to distinguish the mechanism of cell death in BxPC3 cells treated with PC-046. We considered Annexin V-stained (singly) cells to be undergoing early apoptosis and dual Annexin V and PI-stained cells to be undergoing necrosis. At the highest concentration used (1500 nM), we observed cell death by a combination of apoptosis and necrosis (Fig. 7).

**Macromolecule Synthesis.** We saw no selective inhibition of synthesis of DNA, RNA, or protein by PC-046, i.e., the inhibition of cell growth by PC-046 was not preferentially due to the inhibition of DNA synthesis, RNA synthesis, or protein synthesis. These studies were performed at 24 to 72 h. The IC<sub>50</sub> for inhibition of synthesis of each macromolecule averaged approximately 3  $\mu$ M at 72 h (data not shown).

**Pharmacokinetic Studies.** The pharmacokinetics of PC-046 was studied in mice that were given a single intravenous tail vein injection of 88 mg/kg PC-046. The mean (S.D.) peak plasma concentration of 10.8 (4.26)  $\mu$ M was obtained at the





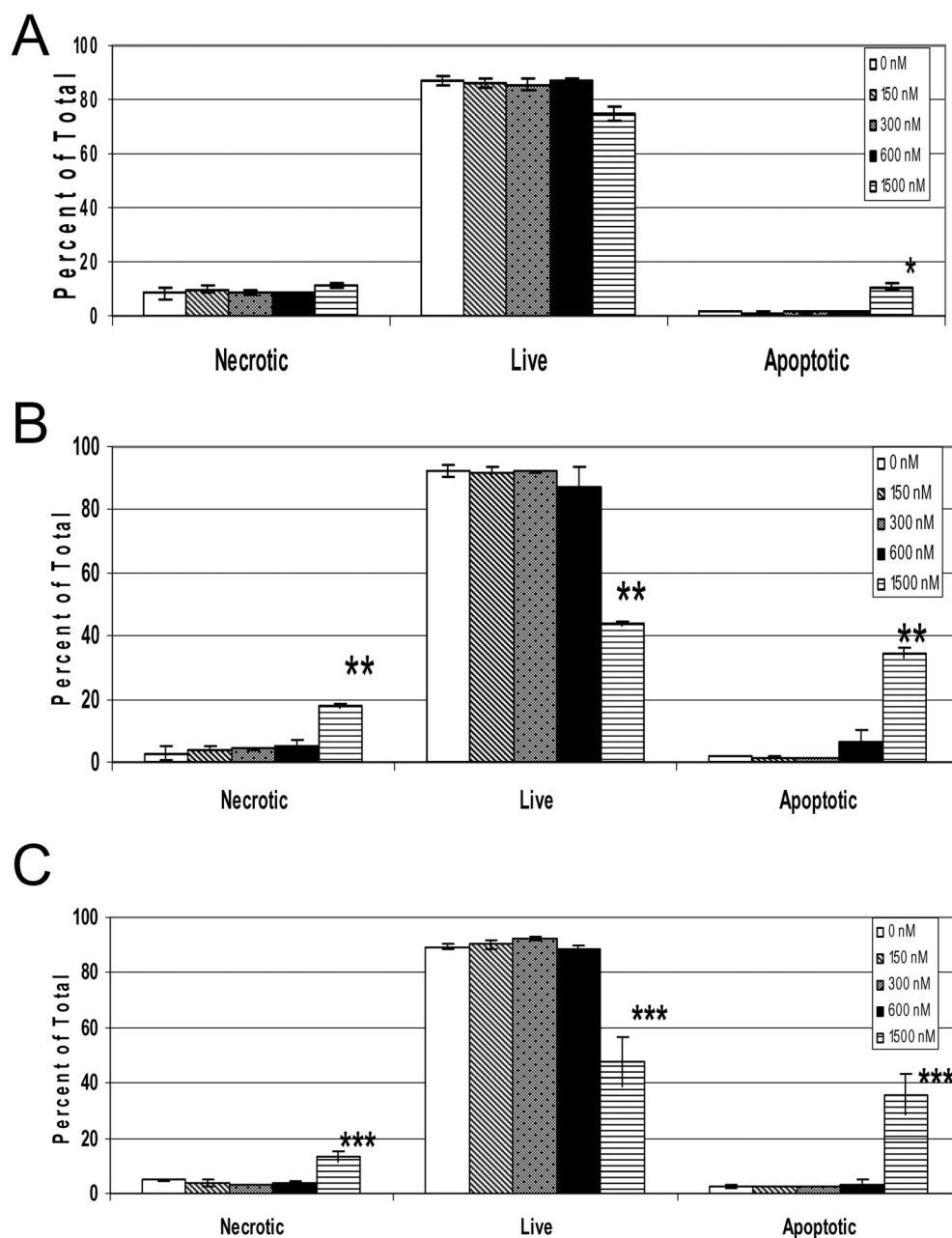
**Fig. 6.** PC-046 causes a block in S- and G<sub>2</sub>/M-phases in BxPC3 *DPC-4(-/-)* cells. BxPC3 *DPC-4(-/-)* cells were treated for 24 (A), 48 (B), or 72 h (C) with increasing concentrations of PC-046. Cell cycle was measured by PI staining and analyzed by flow cytometry. The percentage of cells in cell cycle phases are shown. Mean  $\pm$  S.E.M.,  $n = 3$ . Statistically different from untreated group at \*,  $p < 0.05$ ; \*\*,  $p < 0.01$ ; \*\*\*,  $p < 0.005$ ; \*\*\*\*,  $p < 0.001$ .

first sampling time (1 min). The drug was still detectable in the plasma at the last sampling time of 24 h, with a mean (S.D.) concentration of 0.226 (0.104)  $\mu\text{M}$ . A monoexponential half-life of 7.5 h was observed in mouse plasma, and the AUC was 5.9  $\text{h} \cdot \mu\text{g}/\text{ml}$ . This relatively long half-life could be explained by a low clearance (14.9 l/h/kg) and a large apparent volume of distribution (135.2 l/kg). PC-046 was 91% bound to plasma proteins in mouse plasma and 85% bound in human plasma at a plasma concentration of 3.27  $\mu\text{M}$ . These results suggest extensive binding to tissues.

**Stability Studies.** LC-MS was used to evaluate the stability of PC-046 kept at  $-20^\circ\text{C}$  or at  $22^\circ\text{C}$ , unprotected from light. After 2 years of storage, there was a measurable (8.6%) loss of parent compound when stored at  $-20^\circ\text{C}$  in the dark

and a 43.6% loss at  $22^\circ\text{C}$  in light. We are currently evaluating whether the degradation we observed is due to temperature or light or a combination.

**Antitumor Efficacy Studies.** Studies of antitumor efficacy were performed in SCID mice with human MiaPaCa-2 cells in Matrigel implanted subcutaneously in the front flank. An initial dose-ranging study evaluated a 5 consecutive daily administration of 44 or 66 mg/kg/day PC-046. The 66 mg/kg/day dose was not tolerated ( $>15\%$  weight loss, 60% death) so an intermediate dose of 55 mg/kg/day, daily for 5 days, was evaluated. This dose resulted in substantial (10%) weight loss but reduced MiaPaCa-2 tumor growth compared with untreated controls (preliminary data not shown). In a more definitive experiment comparing 44 or 55 mg/kg/day PC-046



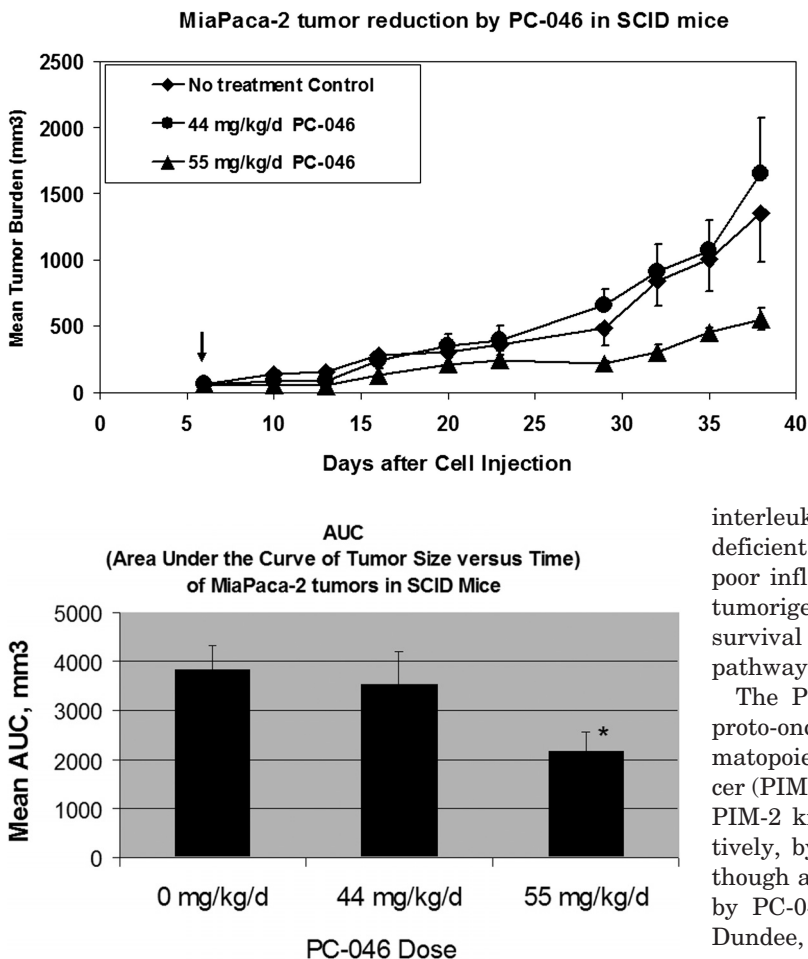
**Fig. 7.** PC-046 causes both early apoptotic and necrotic cell death in BxPC3 *DPC-4(-/-)* cells. BxPC3 *DPC-4(-/-)* cells were treated for 24 (A), 48 (B), or 72 h (C) with increasing concentrations of PC-046. Percentage of necrotic, viable, and early apoptotic cells was measured by dual labeling using Annexin V-Alexa Fluor 488, and PI and analyzed by flow cytometry. Mean  $\pm$  S.E.M.,  $n = 3$ . Statistically different from untreated group at \*,  $p < 0.002$ ; \*\*,  $p < 0.001$ ; \*\*\*,  $p < 0.01$ .

administered daily for 5 days, we saw significant inhibition of MiaPaCa-2 tumor growth compared with the untreated group (Fig. 8). This was associated with a statistically significant reduction in the area under the tumor size  $\times$  time curve compared with controls ( $p < 0.014$ ) (Fig. 9) in the 55 mg/kg/day PC-046-treated group. However, the lower 44 mg/kg/day dose was not effective. It is noteworthy that, although the mice in the 55 mg/kg/day group lost an average of 15.8% of their body weight while they were receiving PC-046 injections, their body weight had recovered by the end of the study.

### Discussion

There are two clear distinctions in this chemical analog development program. 1) There was no improvement in the

selectivity of the PC series analogs for BxPC3 *DPC-4(-/-)* pancreas cancer cells, and 2) the kinesin-specific inhibitory pattern of the lead analog UA-62784 was not replicated. The current PC series does not yield specific SAR information on improved selectivity for the pancreatic cancer-specific *DPC-4* phenotype. Indeed, only a few of the synthesized analogs had selectivity factors in the range of the lead analog UA-62784, which was only 2-fold. None of the analogs significantly improved on that relatively low selectivity ratio. Thus, it remains an open question whether such single-gene selectivity is possible within the context of a limited small molecule-screening program. With regard to the kinesin inhibitory activity, only two PC analogs (PC-042 and PC-053) exhibited inhibitory activity for the molecular target, mitotic kinesin CENP-E, of UA-62784. Overall, there was no clear correlation with cell growth inhibition and kinesin inhibition among



**Fig. 9.** AUC of tumor size versus time of MiaPaca-2 tumors in SCID mice. The AUC of each individual mouse was calculated (days 6 to 23) and then averaged. Results are mean  $\pm$  S.E.M. Statistically different from no treatment group at \*,  $p < 0.014$ .

the 23 compounds surveyed for inhibitory activity against the five kinesins tested (four mitotic and one neuronal).

The lead analog PC-046 inhibited a number of tumor-related protein kinases, with the most potent inhibition against TrkB, IRAK-4, and PIM-1. Overall, TrkB was the most sensitive kinase inhibited by PC-046. The tropomyosin-related kinase TrkB is the receptor tyrosine kinase for the neurotrophic ligand, brain-derived neurotrophic factor (Geiger and Peeper, 2007). The physiologic role of TrkB includes survival signaling for development and function of the nervous system and for suppressing anoikis or cell detachment-mediated apoptosis. The latter feature renders cancer cells highly tumorigenic and metastatic, and TrkB is often found to be overexpressed in several types of aggressive cancers, including pancreatic cancer (Sclabas et al., 2005), prostate cancer, lymphoma, and neuroblastoma (Desmet and Peeper, 2006). Inhibiting TrkB kinase activity is sufficient to block the suppression of anoikis (Geiger and Peeper 2007). This suggests that PC-046 could potentially induce apoptosis in circulating metastatic tumor cells.

The next most sensitive kinase, IRAK-4, is one of the interleukin-1 receptor tyrosine kinase family members that mediate signaling from ligands interacting with the Toll-like receptor (Huang et al., 2005). IRAK-4 seems to mediate nuclear factor- $\kappa$ B activation in the inflammatory response to

**Fig. 8.** Antitumor efficacy of PC-046 in SCID mice.  $10 \times 10^6$  MiaPaca-2 cells in MatriGel were implanted subcutaneously into the flanks of SCID mice. Mice were randomized on day 6 (arrow) and then injected with vehicle alone or 44 or 55 mg/kg/day PC-046 intraperitoneally daily for 5 consecutive days. Mean tumor burden is shown. Mean  $\pm$  S.D. ( $n = 4$  or 5).

interleukin-1 or lipopolysaccharide stimulation. Individuals deficient in IRAK-4 have multiple infections characterized by poor inflammatory responses. A specific role for IRAK-4 in tumorigenesis has not been delineated but might involve cell survival signaling through activation of the nuclear factor- $\kappa$ B pathway.

The PIM serine/threonine kinase family includes three proto-oncogene members that have been associated with hematopoietic cancers (PIM-1 and PIM-2) and pancreatic cancer (PIM-3) (Li et al., 2006). In the current study, PIM-1 and PIM-2 kinase activities were inhibited 68 and 8%, respectively, by PC-046. It is noteworthy that PIM-3 kinase, although associated with pancreatic cancer, was not inhibited by PC-046 (Millipore Kinase Profiler; Millipore UK Ltd, Dundee, UK). When the PIM kinases are overexpressed in cancer cells, apoptosis is inhibited by PIM-kinase-induced phosphorylation of the proapoptotic protein Bad. This allows Bad to liberate the antiapoptotic proteins Bcl-X<sub>L</sub> and Bcl-2. These properties could explain why a PIM-kinase inhibitor such as PC-046 might have antitumor properties (Li et al., 2006). However, the kinase inhibitory activity of PC-046 was not limited to these three kinases, and many other kinases with relevance to cancer were inhibited by >50%, including SRC (Rous sarcoma oncogene cellular homolog), PDGFR $\alpha$  and PDGFR $\beta$ , KDR (kinase insert domain receptor, VEGF), FLT-1 (Fms-related tyrosine kinase 1), DYRK1 $\alpha$  (dual-specificity Tyr phosphorylation-regulated kinase 1A), c-KIT (cytokine stem cell factor receptor), p38 $\alpha$ , AKT-2 (V-akt murine thymoma viral oncogene homolog 2), and ABL-1 (v-abl Ableson leukemia oncogene cellular homolog) (Fig. 7). Indeed, the breadth of kinases inhibited and the inhibition of both tyrosine and serine/threonine kinases suggests that PC-046 has broad-spectrum kinase inhibitory activity. This breadth of activity may also explain an apparent discrepancy between the IC<sub>50</sub> for PC-046-induced cell growth inhibition (7.5 nM; Table 2) and the IC<sub>50</sub>s determined when assayed in the cell-free kinase activity assays (13.4  $\mu$ M for TrkB, 15.4  $\mu$ M for IRAK-4, and 19.1  $\mu$ M for PIM-1). In our cell growth inhibition assays, the addition of PC-046 has multiple consequences, i.e., downstream effects, resulting in multiple kinases being targeted simultaneously. However, in a cell-free system where the activity of a single purified enzyme is used to measure the incorporation of [<sup>33</sup>P]ATP into a specific substrate, a higher amount of the drug is necessary to have

similar effects. In this scenario, because only one kinase is assayed at a time, the contribution of additive or synergistic kinase inhibition on cell growth is underestimated.

It is important that the lead compound PC-046 demonstrated antitumor efficacy *in vivo* in a human pancreatic tumor model in SCID mice. Furthermore, drug concentrations shown to be growth-inhibitory *in vitro* were measured in the plasma of mice that were given tolerable doses of the drug. The relatively long plasma half-life of 7.5 h is also favorable for further development of PC-046 because half-lives for the drug in humans might be estimated at several-fold longer than 7.5 h based on known allometric scaling models (Boxenbaum and Ronfeld, 1983). Further testing of the compound using continuous oral dosing, as done for most existing kinase inhibitors, might further improve antitumor efficacy. Studies are underway to evaluate the oral bioavailability of the compound and to identify its dose-limiting toxicity.

#### Acknowledgments

We thank the Flow Cytometry Service, the Analytical Core Service, and the Experimental Mouse Service at the Arizona Cancer Center and the Mass Spectrometry Core Facility of the University of Arizona Chemistry Department.

#### References

- Boxenbaum H and Ronfeld R (1983) Interspecies pharmacokinetic scaling and the Dedrick plots. *Am J Physiol* **245**:R768–R775.
- Burris H 3rd and Rocha-Lima C (2008) New therapeutic directions for advanced pancreatic cancer: targeting the epidermal growth factor and vascular endothelial growth factor pathways. *Oncologist* **13**:289–298.
- Collins PJ, Hennessy LK, Leibelt CS, Roby RK, Reeder DJ, and Foxall PA (2004) Developmental validation of a single-tube amplification of the 13 CODIS STR loci, D2S1338, D19S433, and amelogenin: the AmpFISTR Identifier PCR Amplification Kit. *J Forensic Sci* **49**:1265–1277.
- Darzynkiewicz Z, Gong J, Juan G, Ardel B, and Traganos F (1996) Cytometry of cyclin proteins. *Cytometry* **25**:1–13.
- Desmet CJ and Peeper DS (2006) The neurotrophic receptor TrkB: a drug target in anti-cancer therapy? *Cell Mol Life Sci* **63**:755–759.
- Funk CJ, Davis AS, Hopkins JA, and Middleton KM (2004) Development of high-throughput screens for discovery of kinesin adenosine triphosphatase modulators. *Anal Biochem* **329**:68–76.
- Geiger TR and Peeper DS (2007) Critical role for TrkB kinase function in anoikis suppression, tumorigenesis, and metastasis. *Cancer Res* **67**:6221–6229.
- Guha SK, Wu B, Kim BS, Woonphil B, and Koo S (2006) TMS-OTf-catalyzed  $\alpha$ -bromination of carbonyl compounds by *N*-bromosuccinimide. *Tetrahedron Lett* **47**: 291–293.
- Henderson MC, Shaw YJ, Wang H, Han H, Hurley LH, Flynn G, Dorr RT, and Von Hoff DD (2009) UA62784, a novel inhibitor of centromere protein E kinesin-like protein. *Mol Cancer Ther* **8**:36–44.
- Hirokawa N and Noda Y (2008) Intracellular transport and kinesin superfamily proteins, KIFs: structure, function, and dynamics. *Physiol Rev* **88**:1089–1118.
- Holub JM, O'Toole-Colin K, Getzel A, Argenti A, Evans MA, Smith DC, Dalglish GA, Rifat S, Wilson DL, Taylor BM, et al. (2004) Lipid-lowering effects of ethyl 2-phenacyl-3-aryl-1*H*-pyrrole-4-carboxylates in rodents. *Molecules* **9**:134–157.

- Huang YS, Misiar A, and Li LW (2005) Novel role and regulation of the interleukin-1 receptor associated kinase (IRAK) family proteins. *Cell Mol Immunol* **2**:36–39.
- Hunter AW, Caplow M, Coy DL, Hancock WO, Diez S, Wordeman L, and Howard J (2003) The kinesin-related protein MCAK is a microtubule depolymerase that forms an ATP-hydrolyzing complex at microtubule ends. *Mol Cell* **11**:445–457.
- Jaffee EM, Hruban RH, Canto M, and Kern SE (2002) Focus on pancreas cancer. *Cancer Cell* **2**:25–28.
- Jemal A, Siegel R, Ward E, Hao Y, Xu J, Murray T, and Thun MJ (2008) Cancer statistics, 2008. *CA Cancer J Clin* **58**:71–96.
- Jones S, Zhang X, Parsons DW, Lin JC, Leary RJ, Angenendt P, Mankoo P, Carter H, Kamiyama H, Jimeno A, et al. (2008) Core signaling pathways in human pancreatic cancers revealed by global genomic analyses. *Science* **321**:1801–1806.
- Li YY, Popivanova BK, Nagai Y, Ishikura H, Fujii C, and Mukaida N (2006) Pim-3, a proto-oncogene with serine/threonine kinase activity, is aberrantly expressed in human pancreatic cancer and phosphorylates bad to block bad-mediated apoptosis in human pancreatic cancer cell lines. *Cancer Res* **66**:6741–6747.
- Lieber M, Mazzetta J, Nelson-Rees W, Kaplan M, and Todaro G (1975) Establishment of a continuous tumor-cell line (panc-1) from a human carcinoma of the exocrine pancreas. *Int J Cancer* **15**:741–747.
- Lombillo VA, Nislow C, Yen TJ, Gelfand VI, and McIntosh JR (1995) Antibodies to the kinesin motor domain and CENP-E inhibit microtubule depolymerization-dependent motion of chromosomes *in vitro*. *J Cell Biol* **128**:107–115.
- Meanwell NA, Romine JL, Rosenfeld MJ, Martin SW, Trehan AK, Wright JJ, Malley MF, Gougoutas JZ, Brassard CL, and Buchanan JO (1993) Nonprostanoid prostacyclin mimetics. 5. Structure-activity relationships associated with [3-[4-(4,5-diphenyl-2-oxazolyl)-5-oxazolyl]phenoxy]acetic acid. *J Med Chem* **36**:3884–3903.
- Miyaki M and Kuroki T (2003) Role of Smad4 (*DPC4*) inactivation in human cancer. *Biochem Biophys Res Commun* **306**:799–804.
- Mosmann T (1983) Rapid colorimetric assay for cellular growth and survival: application to proliferation and cytotoxicity assays. *J Immunol Methods* **65**:55–63.
- Nicolaou KC, Hao J, Reddy MV, Rao PB, Rassias G, Snyder SA, Huang X, Chen DY, Brenzovich WE, Giuseppone N, et al. (2004) Chemistry and biology of diazomide A: second total synthesis and biological investigations. *J Am Chem Soc* **126**:12897–12906.
- Nislow C, Lombillo VA, Kuriyama R, and McIntosh JR (1992) A plus-end-directed motor enzyme that moves antiparallel microtubules *in vitro* localizes to the interzone of mitotic spindles. *Nature* **359**:543–547.
- Sawin KE, LeGuellec K, Philippe M, and Mitchison TJ (1992) Mitotic spindle organization by a plus-end-directed microtubule motor. *Nature* **359**:540–543.
- Sclabas GM, Fujioka S, Schmidt C, Li Z, Frederick WA, Yang W, Yokoi K, Evans DB, Abbruzzese JL, Hess KR, et al. (2005) Overexpression of tropomyosin-related kinase B in metastatic human pancreatic cancer cells. *Clin Cancer Res* **11**:440–449.
- Tan MH, Nowak NJ, Loor R, Ochi H, Sandberg AA, Lopez C, Pickren JW, Berjian R, Douglass HO Jr, and Chu TM (1986) Characterization of a new primary human pancreatic tumor line. *Cancer Invest* **4**:15–23.
- Tascilar M, Skinner HG, Rosty C, Sohn T, Wilentz RE, Offerhaus GJ, Adsay V, Abrams RA, Cameron JL, Kern SE, et al. (2001) The SMAD4 protein and prognosis of pancreatic ductal adenocarcinoma. *Clin Cancer Res* **7**:4115–4121.
- Vermes I, Haanen C, Steffens-Nakken H, and Reutelingsperger C (1995) A novel assay for apoptosis. Flow cytometric detection of phosphatidylserine expression on early apoptotic cells using fluorescein labelled annexin V. *J Immunol Methods* **184**:39–51.
- Wang H, Han H, and Von Hoff DD (2006) Identification of an agent selectively targeting *DPC4* (deleted in pancreatic cancer locus 4)-deficient pancreatic cancer cells. *Cancer Res* **66**:9722–9730.
- Yang Z and Goldstein LS (1998) Characterization of the KIF3C neural kinesin-like motor from mouse. *Mol Biol Cell* **9**:249–261.
- Yen TJ, Compton DA, Wise D, Zinkowski RP, Brinkley BR, Earnshaw WC, and Cleveland DW (1991) CENP-E, a novel human centromere-associated protein required for progression from metaphase to anaphase. *EMBO J* **10**:1245–1254.
- Yunis AA, Arimura GK, and Rassin DJ (1977) Human pancreatic carcinoma (Mi-aPaCa-2) in continuous culture: sensitivity to asparaginase. *Int J Cancer* **19**:128–135.

**Address correspondence to:** Dr. Robert T. Dorr, Arizona Cancer Center, 1515 N. Campbell Ave, Tucson, AZ 58724. E-mail: bdorr@azcc.arizona.edu